Coordinating Energy Management Systems in Smart Cities with Electric Vehicles

Mohamed Lotfi [a,b], Tiago Almeida [a], Mohammad S. Javadi [b], Gerardo J. Osório [c], Cláudio Monteiro [a], João P. S. Catalão [a,b,*]

[a] *Faculty of Engineering of the University of Porto (FEUP), R. Dr. Roberto Frias, 4200-465, Porto, Portugal*
[b] *INESC TEC, R. Dr. Roberto Frias, 4200-465, Porto, Portugal*
[c] *University Portucalense Infante D. Henrique (UPT), R. Dr. António Bernardino de Almeida, 541, Porto Portugal*
**catalao@fe.up.pt*

Abstract

The rapid proliferation of Electric Vehicles (EVs) creates an inherent link between the previously independent transport and power sectors. This is especially relevant in the smart cities paradigm, which focuses on optimizing resource management using modern software tools and communication infrastructures. The optimal management of energy resources is of key importance, and with mobile EVs playing a pivotal role in smart city power flows, the coordination of energy management systems (EMSs) at their parking locations can bear global benefits. In this study the coordination between home energy management systems (HEMSs) and EV parking lot management systems (PLEMS) is proposed, modeled, and simulated, as a new contribution to earlier studies. The EMSs coordinate through partially sharing individual EV schedules and without sharing private information. Missing information is completed through public cloud repositories and services. The HEMS and PLEMS are implemented using mixed-integer linear programming (MILP). The proposed coordination framework is computationally implemented and simulated based on a real-life case study. The results show that the proposed EMS coordination framework is both technically beneficial for power grids and economically beneficial for EV owners.

Keywords: Energy Management Systems; Electric Vehicles; Smart Cities; Optimization.

Nomenclature

List of Acronyms and Abbreviations	
ANN	Artificial Neural Network
BTE	Special Low Voltage (*Baixa Tensão Normal*)
BTN	Normal Low Voltage (*Baixa Tensão Especial*)
DER	Distributed Energy Resources
DG	Distributed Generation
DI	Discomfort Index
DR	Demand Response
DSM	Demand Side Management

DSO	Distribution System Operator
EMS	Energy Management System
ERSE	Portuguese Energy Regulation Services Entity (*Entidade Reguladora dos Serviços Energéticos*)
ESS	Energy Storage System
EV	Electric Vehicle
EVPL	Electric Vehicle Parking Lot
GEMS	Grid Energy Management System
HEMS	Home Energy Management System
IoT	Internet of Things
ISO	Independent System Operator
MILP	Mixed Integer Linear Programming
MIP	Mixed Integer Programming
MPC	Model Predictive Control
MPPT	Maximum Power Point Tracking
MV	Medium Voltage
PL	Parking Lot
PLEMS	Parking Lot Energy Management System
PV	Photovoltaic
RES	Renewable Energy Resources
SG	Smart Grid
TSO	Transmission System Operator
List of Variables and Indices used to model the PLEMS	
ΔT^{PL}	Time increment (timeslot size) for the PLEMS [h]
NT^{PLEMS}	Number of timeslots in a 24-hour period for the PLEMS [-]
N_t^{PL}	Number of EVs stationed at the PL during timeslot *t* [-]
N_t^{arr}	Number of EVs arriving at the PL at timeslot *t* [-]
N_t^{dep}	Number of EVs departing from the PL at timeslot *t* [-]
N^{EVPL}	Total number of EVs using the PL [-]
$EVID$	Index for each individual EV using the PL [-]
Φ_t^{EVID}	Binary variable indicating whether EVID is stationed in the PL at timeslot *t* [-]
$TARRPL_{EVID}$	Arrival timeslot of *EVID* at the PL [-]
$TDEPPL_{EVID}$	Departure timeslot of *EVID* from the PL [-]
E_t^{PL}	Total aggregated energy stored by the PL at timeslot *t* [kWh]
E_t^{EVID}	Energy stored (state-of-energy) for *EVID* at timeslot *t* [kWh]
$E_t^{PL,cap}$	Maximum energy storage capacity of the PL at timeslot *t* [kWh]
$E_t^{EVID,cap}$	Maximum energy storage capacity (maximum state-of-energy) for *EVID* at timeslot *t* [kWh]
SOC_t^{EVID}	State-of-Charge of *EVID* at timeslot *t* [-]
SOC_t^{PL}	State-of-Charge of the PL at timeslot *t* [-]
P_t^{G2PL}	Total power injected from the grid to the PL at timeslot *t* [kW]
$P_t^{G2PL,en}$	Power injected from the grid to the PL for energy purchased at timeslot *t* [kW]
$P_t^{G2PL,reg,down}$	Power injected from the grid to the PL for regulation-down offer at timeslot *t* [kW]
P_t^{PL2G}	Total power injected from the PL to the grid at timeslot *t* [kW]
$P_t^{PL2G,en}$	Power injected from the PL to the grid for energy sold at timeslot *t* [kW]
$P_t^{PL2G,reg,up}$	Power injected from the PL to the grid for regulation-up offer at timeslot *t* [kW]
$P_t^{PL2G,res}$	Power injected from the PL to the grid for reserve market offer at timeslot *t* [kW]
$\mathbf{FPL2G_t}$	Binary variable indicating whether power is being injected from the PL to the grid at timeslot *t* [-]
$\mathbf{FG2PL_t}$	Binary variable indicating whether power is being injected from the grid to the PL at timeslot *t* [-]
P_t^{PV2PL}	Power injected from the rooftop PV installations to the PL at timeslot *t* [kW]
$\gamma^{PL,ch}$	Maximum charging rate of the PL [kW]
$\gamma^{PL,dis}$	Maximum discharging rate of the PL [kW]
E_t^{arr}	Aggregated energy of EVs arriving to the PL at timeslot *t* [kWh]
E_t^{dep}	Aggregated energy of EVs departing from the PL at timeslot *t* [kWh]
$\eta_t^{PL,ch}$	Charging efficiency of EVs parked in the PL at timeslot *t* [-]
$\eta_t^{PL,dis}$	Discharging efficiency of EVs parked in the PL at timeslot *t* [-]
$SOC_t^{EVID,up}$	State-of-Charge increment of EVID at timeslot *t* [-]

$SOC_t^{EVID,down}$	State-of-Charge decrement of EVID at timeslot *t* [-]
$SOC_t^{EVID,dep}$	Scheduled departure SoC of EVID at timeslot *t* [-]
SOC_t^{up}	State-of-Charge increment for the PL at timeslot *t* [-]
SOC_t^{down}	State-of-Charge decrement for the PL at timeslot *t* [-]
$Profit^{EVPL}$	Total profit of the PL for the 24-ahead decision-making horizon [€]
List of Variables and Indices used to model the HEMS	
ΔT^{HEMS}	Time increment (timeslot size) for the HEMS [h]
NT^{HEMS}	Number of timeslots in a 24-hour period for the HEMS [-]
P_t^{G2H}	Power injected from the grid to the home (for energy bought) at timeslot *t* [kW]
P_t^{H2G}	Power injected from the home to the grid (for energy sold) at timeslot *t* [kW]
N^{shift}	Number of shiftable loads (appliances) for the HEMS [-]
$LB_{i,b}$	Baseline (before HEMS implementation) lower bound (timeslot) of appliance *i* operating interval [-]
$UB_{i,b}$	Baseline (before HEMS implementation) upper bound (timeslot) of appliance *i* operating interval [-]
$B_{i,t}$	Binary variable indicating whether appliance *i* is operating at timeslot t before HEMS implementation [-]
$LB_{i,s}$	User-defined (after HEMS implementation) lower bound (timeslot) of appliance *i* operating interval [-]
$UB_{i,s}$	User-defined (after HEMS implementation) upper bound (timeslot) of appliance *i* operating interval [-]
$S_{i,t}$	Binary variable indicating whether appliance *i* is operating at timeslot *t* after HEMS implementation [-]
P_t^{HBase}	Base (unshiftable) load for the home at timeslot *t* [kW]
P_t^{HD}	Total power demand for the home at timeslot *t* [kW]
$P_t^{HESS,ch}$	Charging power of the home ESS at timeslot *t* [kW]
$P_t^{HESS,dis}$	Discharging power of the home ESS at timeslot *t* [kW]
$\mathbf{ESSCH}_t$	binary variable indicating whether the home ESS is charging at timeslot *t* [-]
$\mathbf{ESSDIS}_t$	binary variable indicating whether the home ESS is discharging at timeslot *t* [-]
$\gamma^{HESS,ch}$	maximum charging rate of the home ESS [kW]
$\gamma^{HESS,dis}$	maximum discharging rate of the home ESS [kW]
E_t^{HESS}	energy stored by the home ESS at timeslot *t* [kWh]
$E^{HESS,Cap}$	maximum energy storage capacity of the home ESS [kWh]
$\eta^{HESS,ch}$	charging efficiency of the home ESS [-]
$\eta^{HESS,dis}$	discharging efficiency of the home ESS [-]
SOC_t^{HESS}	State-of-Charge of the home ESS at timeslot *t* [-]
$SOC^{HESS,min}$	Minimum allowable SoC for the home ESS [-]
$SOC^{HESS,max}$	Maximum allowable SoC for the home ESS [-]
P_t^{HPV}	Total power generated by the home PV panels at timeslot *t* [kW]
P_t^{HPV2H}	Power generated by the home PV panels and self-consumed at timeslot *t* [kW]
P_t^{HPV2G}	Power generated by the home PV panels and sold to the grid at timeslot *t* [kW]
Variables and Indices used to model the coordination between the HEMS and the PLEMS	
$t^{EVID,arr,PL}$	Time of arrival of *EVID* at the PL [h]
$t^{EVID,dep,H}$	Time of departure of *EVID* from home [h]
$t^{EVID,arr,H}$	Time of arrival of *EVID* at home [h]
$t^{EVID,dep,PL}$	Time of departure of *EVID* from the PL [h]
$TCOM^{EVID,2PL}$	Commuting time of *EVID* from home to the PL [h]
$TCOM^{EVID,2H}$	Commuting time of *EVID* from the PL to home [h]
$SOC^{EVID,arr,PL}$	State-of-Charge of *EVID* when arriving at the PL [-]
$SOC^{EVID,arr,H}$	State-of-Charge of *EVID* when arriving at home [-]
$SOC^{EVID,dep,H}$	State-of-Charge of *EVID* when departing from home [-]
$SOC^{EVID,dep,PL}$	State-of-Charge of *EVID* when departing from the PL [-]
$\Delta SOC^{EVID,2PL}$	State-of-Charge lost by *EVID* during the commute to the PL [-]
$\Delta SOC^{EVID,2H}$	State-of-Charge lost by *EVID* during the commute to home [-]
$DCOM^{EVID,2PL}$	Distance driven by *EVID* from home to the PL [km]
$DCOM^{EVID,2H}$	Distance driven by *EVID* from the PL to home [km]
$\eta^{drive,EVID}$	Driving efficiency of *EVID* [1/km]

1. Introduction

1.1 Background and Motivation: The Smart Cities Paradigm

Accelerated transition towards smart cities can clearly be observed globally. Severe environmental alerts combined with exponential growth of human populations (and urban population densities) makes it imperative to develop sustainable cities to manage resources as efficiently as possible [1].

With modern day crises being mainly due to inefficient management of resources, smart cities are no longer seen as a luxury, but a necessity for the sustained wellbeing of humanity. The cornerstones of any smart city are 1) the employment of Internet-of-Things (IoT)-enabling to collect data, 2) to use the collected data to optimize the resource management efficiency, and 3) iterate this process to improve the design of the processes by which resources are allocated and used [2].

Indeed, the development of an IoT infrastructure has been a key enabler of the transition towards smart cities. The other key enabler is cloud computing, allowing data to be stored, accessed, and processed by different users simultaneously [3]. While the development of smart cities impacts all sectors, some are more affected than others. The electrical power and transport sectors are being heavily impacted by this transition. In fact, both sectors are becoming increasingly intertwined in this new paradigm [4].

1.2 The Intertwining of Electric Power and Transport Sectors

The electric power sector has seen many profound changes in the past few decades. Concerns over security of supply have led a wave of electricity market liberalization and the activation of demand-side management (DSM) policies. In this competitive electricity market, distributed energy resources (DERs) became valuable assets in the demand-side. Typically, local DERs are small-scale distributed generation (DG) and energy storage systems (ESSs) [5].

More recently, with the urgency of minimizing greenhouse gas emissions, renewable energy sources (RESs) have become the preferred means of generating electricity, both on the demand-side (e.g., DERs) and on the generation utilities side (e.g., wind and solar farms). Meanwhile, the same government climate actions which mandated shifting to cleaner energy production have also affected another emission-heavy sector: the transport sector. Electrification of transport, particularly the proliferation of Electric Vehicles (EVs), has been at the forefront of this change [6].

At the same time, transport electrification inherently creates an everlasting link between the electric power and transport sectors, with the latter now becoming a major component of the demand-side and DSM. In fact, EVs intersect multiple elements of smart cities: connection to the power grid as a DER, asset of final energy users as citizen-owned vehicles for personal transport, using road and transit infrastructure, and dependence on cloud services such as navigation services, traffic and weather data, electricity prices, etc. This is illustrated in Fig. 1.

The simultaneous proliferation of RESs and EVs has been proven (both in literature and in real-life) to successfully reduce emissions significantly [7]. On the one hand: EVs eliminate local emissions of their combustion engine counterparts, while on the other hand charging their batteries from electricity generated by low-emission sources due to high levels of RESs.

However, having a high penetration of DERs and EVs causes multiple technical challenges in the operation of the electrical power grid. While modern smart grids (SG) are designed taking into account this fact, critical reliability issues are still encountered if the integration of both is performed in an uncontrolled manner.

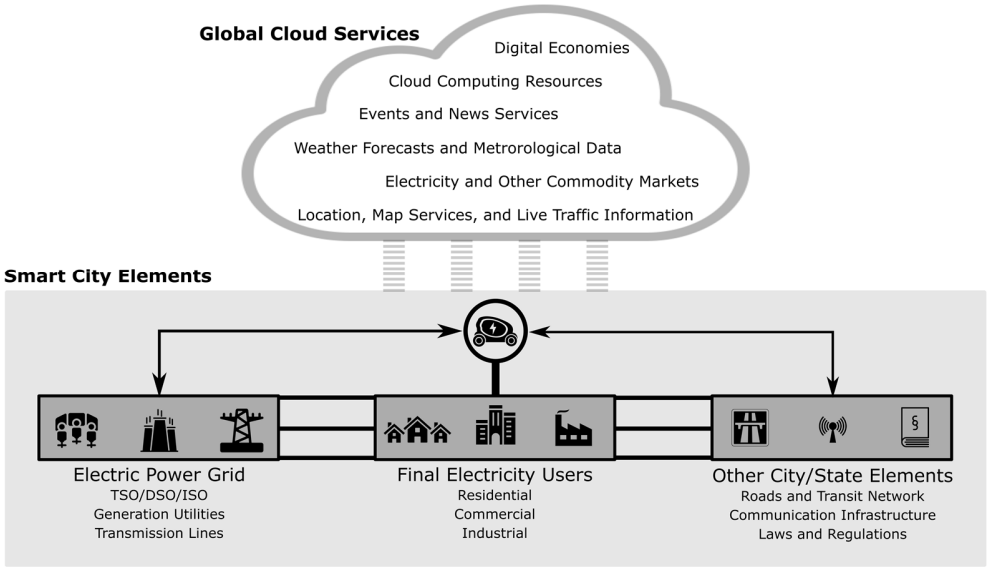

Fig. 1. Elements of a smart city interdependent through the presence of EVs.

Energy Management Systems (EMS) have already been used ever since DSM measures, especially Demand Response (DR) and dynamic pricing policies, were introduced. Their main objective has been to schedule energy consumption in order to make the best of the off-peak low electricity prices. In modern SGs, EMSs are developed accounting for technical constraints of the power grid and therefore they are a great tool to mitigate the technical challenges of high RES and EV penetration, while maintaining the economic incentives to the demand-side.

1.3 State-of-the-Art: Energy Management Systems with Electric Vehicles

Home Energy Management Systems (HEMS) which include EVs have been extensively studied in scientific literature. With accurate modeling, the HEMS scheduling results in decreased electricity bills through optimized utilization of local DERs (PV panels and EVs) and maximizing self-consumption during peak hours, while increasing the grid-independence [8].

A Mixed-Integer Linear Programming (MILP) model for a HEMS was introduced in [9]. The proposed model incorporated an ESS EV, PV, dynamic DR tariffs, and shiftable loads. By considering the homeowners' preferences for the usage time of each

shiftable load, a discomfort index (DI) was calculated as a proportional value to the amount of load shifted. Multi-objective MILP optimization was then used to obtain the day-ahead schedule that provides the optimal tradeoff between minimizing the electricity bill and user discomfort. The results showed that the HEMS scheduling of the DERs and EV provided higher economic benefits for the homeowners through increased self-consumption while contributing to grid stability. Another recent study [10] investigated different operating strategies for another HEMS model, which also considered PV installations, an EV, shiftable loads, an ESS, and dynamic DR tariffs, and reiterated the same findings and conclusions.

A recent study [11] proposed a more complex HEMS model which addressed real-life uncertainties in user behavior and solar generation using a combination of algorithms: Model Predictive Control (MPC), Artificial Neural Networks (ANN), Markov chain, and conditional probability techniques. The analysis performed clearly showed the capability of the HEMS to significantly decrease the electricity bills compared to non-optimized rule-based methods (e.g., homeowners manual scheduling by simply following the dynamic DR tariffs). The paper also presented an important finding by simulating different time resolutions for the HEMS implementation. It was found that decreasing the time resolution from 1 hour to 15 minutes had little impact on the cost savings (<1%), while significantly increasing the computational effort (40x). This sets an important guideline on the choice of the time resolution.

In [4], a novel analysis was presented in which the coordination between the HEMS and the Grid Energy Management System (GEMS) was studied. The two EMSs shared information such as day-ahead driving schedules of the EVs and forecasted power profiles. The paper demonstrated that by coordinating the operation between the HEMS and GEMS, the electricity bills of the homeowners can be further decreased in addition to reduced PV curtailment.

All previous works ([4], [8]–[11]) demonstrated techno-economic benefits of employing HEMSs incorporating EVs and DERs. However, in smart cities with high EV presence, traditional parking lots (PLs) can be converted to grid-connected EVPLs. EVPLs provide parking and charging services to EV owners at an agreed-upon tariff. By aggregating a large number of EVs, they are also capable of making a significant profit by being an ancillary services provider to the grid at a medium-voltage (MV) level. Being commercial establishments, their EMSs have one objective: maximize profits. In addition, the EVPLs make use of installed local generation (rooftop PVs) to further increase their net profits. Accordingly, recent works have proposed models for EVPL EMSs (PLEMSs). Recent studies on PLEMSs are surveyed subsequently.

A dynamic programming algorithm for a PLEMS was proposed in [12]. The intended application was the commercial areas where EVs are parked during power grid's peak hours. By using the aggregated potential of stationed EVs, the PLEMS was capable of determining the optimal charging schedule for each EV, which maximized the owner's profits by providing ancillary services to the grid while committing to the agreed upon charging rate for the total parked duration of each EV.

A PLEMS was implemented in [13] using fuzzy logic inference. In this study, the main focus was not to assess the PL's profitability, but rather its capability to mitigate grid overloading (which would be the case in uncontrolled EV charging at the EVPL) without sacrificing the charging commitments made to the EV owners. The PLEMS was shown to be successful at achieving this goal.

A combined EMS which aimed at maximizing the parking lot owner's profit while minimizing the distribution system operator's (DSO's) costs was proposed in [14]. In this sense, the PL would be incorporated as a subproblem in the GEMS. A stochastic MILP optimization model was used to account for the uncertainty of grid-connected RESs using a weighted-scenario based approach. The results showed that the implemented EMS effectively reduced the DSO's costs while maximizing the EVPL profits. In [15], an EVPL with rooftop PV installations was modeled and a real-time PLEMS was proposed, taking into account power grid constraints and dynamic electricity pricing. The PLEMS determined near-optimal charging/discharging of the parked EVs to increase the EVPL's profit. Building on [14] and [15], a PV-equipped EV parking lot was modeled in [16]. The proposed MILP model for day-ahead operational planning showed that the designed PLEMS significantly increasing the EVPL's profits, without sacrificing neither the EVs' charging requirements, nor the grid constraints. On the contrary, a significant portion of the additional profit came from providing ancillary services to the grid, which enhanced grid reliability and reduced power losses.

1.4 Novel Contributions and Paper Organization

From the conducted literature survey, the following is noted:

- HEMSs have been extensively studied in literature, demonstrating their capability to minimize electricity bills (with minimal sacrifice of comfort) by shifting loads and optimizing EV charging/discharging according to dynamic DR tariffs.
- PLEMSs have been proposed in recent studies, mainly aiming at either maximizing the EVPL's profit or that of the grid operator. The aggregated capacity of parked EVs allow the EVPL to do so by participating in the ancillary services market.
- Only one study [4] considered the coordination between two EMSs (HEMS and the GEMS) in the presence of consumer EVs. No studies were found that studied the simultaneous operation of PLEMSs and HEMSs.

This was identified as a critical gap in literature. Therefore, the **novel contributions** of this paper can be listed as follows:

- Study the effects of coordinating different EMSs employed in a smart city. Particularly, consider a PLEMS with all participating EVs' owners having a HEMS installed at home. Both the EVPL and the homes have local PV installations, and both are connected to a SG with dynamic DR tariffs.
- Investigate the impacts of the EMSs coordinated operation by simulating a real-world case study, including traffic uncertainties affecting transit times, in addition to real PV generation, load profiles, and electricity market data.

- Model the grid using power flow simulations to obtain a complete techno-economic evaluation of different scenarios.
- Investigate synergies that can be obtained through the coordinated operation of different smart city EMSs.

The remainder of the paper is presented as follows. In Section 2, the methodology is presented, including the conceptual model, mathematical formulation and computational implementation. In Section 3, the real-world case study used for the simulations is defined. In Section 4, the results of the simulations are presented and discussed. Recommendations for future work are discussed in Section 5. The conclusions are summarized in Section 6.

2. Methodology

2.1 Conceptual Model

The conceptual model devised for this study is shown in Fig. 2. In this model, residents of different neighborhoods commute daily to an EVPL. The latter has rooftop PV installations and a PLEMS. Individual houses have their own DERs (specifically, PV panels and ESSs) and a HEMS. The EVPL and all houses are connected to the same SG, with dynamic DR electricity prices, bidirectional power flows, and open access to participate in providing ancillary services.

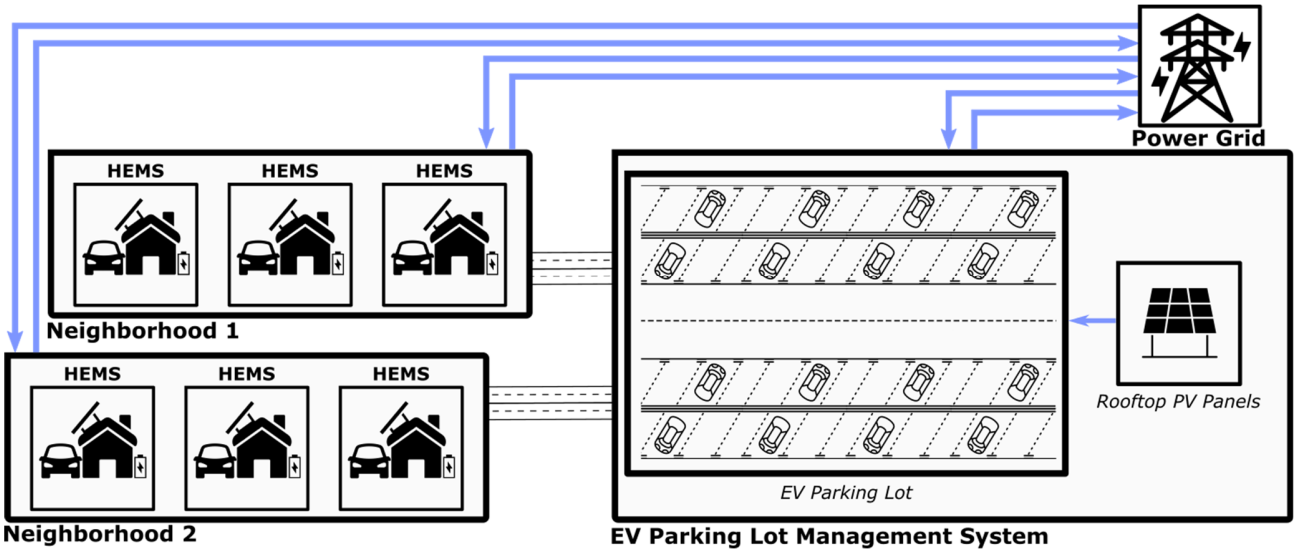

Fig. 2. Conceptual model for the interaction between various EMSs with EVs.

The following scenarios will be studied and compared in this paper:

Scenario 1 – No EMSs: In this (base) scenario, the houses have neither DERs nor an EMS installed. In this case, the houses are "traditional" homes with unscheduled operation of the appliances and uncontrolled charging of the EVs (i.e., once they arrive, they are plugged in until fully charged). In this scenario, the parking lot is nothing more than a parking space for the EVs.

Scenario 2 – HEMS only: In this scenario, the houses are smart homes, with DERs (PV panels and batteries) installed and a HEMS operating to schedule all electricity usage (including EV charging). Each home has its own HEMS. The parking lot still exists only as a parking space for the EVs.

Scenario 3 – PLEMS only: In this scenario, the houses are traditional houses, as they were in Scenario 1. The EVPL is converted to a commercialized smart EVPL, which has its own DERs (rooftop PV panels) and an EMS.

Scenario 4 – All EMSs: In this scenario, both the houses and the parking lot are converted to their smart versions, equipped with DERs and EMSs. In this scenario, the EMSs coordination is studied. The EV owners include their arrival and departure times in the HEMS preferences, which shares this information with the PLEMS. The latter in turn shares back the expected SoC of the EV upon departure from the PL.

The techno-economic benefits of DERs, HEMSs, and PLEMSs, separately, have all been already established in previous studies and in the real world. Since the objective of this study is to investigate the synergies that can be obtained through the coordinated operation of these systems in the presence of EVs, the main comparison to be performed is between scenarios 1 and 4. Moreover, it is important to realize that in real life, the intermediate scenarios (2 and 3) are too idealistic to be true. With high EV penetration and the global progression towards smart cities with widespread DERs, it is almost impossible to imagine a real scenario where PLEMSs exist while HEMSs do not, or vice versa. With this being said, it is important to include scenarios 2 and 3 as control scenarios, to identify if any observation is due to the synergy of the EMSs or if it already results from one of the individual EMSs on its own. The mathematical formulation used to model these scenarios is presented subsequently.

2.2 Parking Lot Energy Management System

The EVPL and its grid interaction are modeled using a MILP formulation. The optimal day-ahead charging and discharging schedule of parked EVs is determined to maximize the EVPL′s profit. The model considers the presence of rooftop PV panels and DR participation to sell energy to the grid or participate in the reserve and regulation markets in response to offers by the independent system operator (ISO). The day-ahead schedule is obtained by discretizing the 24 hours into NT^{PLEMS} time slots of size ΔT^{PL} hours, as shown in (1).

$$\Delta T^{PL} = \frac{24}{NT^{PLEMS}} \tag{1}$$

During each timeslot $t = 1 \dots NT^{PLEMS}$, there are N_t^{PL} EVs parked in the PL, which changes every timeslot as shown in (2).

$$N_t^{PL} = N_{t-1}^{PL} + N_t^{arr} + N_t^{dep} \quad \forall\, t = 1 \dots NT^{PLEMS} \tag{2}$$

In every timeslot there is a number of N_t^{arr} and N_t^{dep} newly arriving and departing EVs, respectively. The total number of EVs which use the PL is expressed as N^{EVPL}, and each individual EV is assigned an index $EVID = 1 \dots N^{EVPL}$. A binary variable Φ_t^{EVID} indicates whether or not an EV $EVID$ is inside the PL during timeslot t or not, as shown in (3).

$$\Phi_t^{EVID} = \begin{cases} 1, & TARRPL_{EVID} \le t \le TDEPPL_{EVID} \\ 0, & otherwise \end{cases} \tag{3}$$
$$\forall\, EVID = 1 \dots N^{EVPL}, t = 1 \dots NT^{PLEMS}$$

Each EV's arrival and departure time to/from the EVPL is expressed as $TARRPL_{EVID}$ and $TDEPPL_{EVID}$, respectively. In (4) the total aggregated stored energy by the EVPL in timeslot t (E_t^{PL}) is calculated as the sum of energy stored of individual batteries of parked EVs (E_t^{EVID}). Similarly, in (5) the maximum storage capacity of the EVPL ($E_t^{PL,cap}$) is the sum of that of all parked EVs ($E_t^{EVID,cap}$). The corresponding SoC of individual EVs and the PL is defined in (6) and (7), respectively.

$$E_t^{PL} = \sum_{EVID=1}^{N^{EVPL}} \left(\Phi_t^{EVID} \cdot E_t^{EVID} \right) \tag{4}$$

$$E_t^{PL,cap} = \sum_{EVID=1}^{N^{EVPL}} \left(\Phi_t^{EVID} \cdot E_t^{EVID,cap} \right) \tag{5}$$

$$SOC_t^{EVID} = \frac{E_t^{EVID}}{E_t^{EVID,cap}} \tag{6}$$
$$\forall\, EVID = 1 \dots N^{EVPL}, \forall\, t = 1 \dots NT^{PLEMS}$$

$$SOC_t^{PL} = \frac{E_t^{PL}}{E_t^{PL,cap}} \tag{7}$$
$$\forall\ t = 1 \dots NT^{PLEMS}$$

For each timeslot, the total power injected from the grid to the PL and the total power injected from the PL to the grid are expressed in (8) and (9), respectively.

$$P_t^{G2PL} = P_t^{G2PL,en} + P_t^{G2PL,reg,down} \tag{8}$$

$$P_t^{PL2G} = P_t^{PL2G,en} + P_t^{PL2G,reg,up} + P_t^{PL2G,res} \tag{9}$$

In (8), the total power injected to the PL (P_t^{G2PL}) is equal to that corresponding to the energy purchased from the grid ($P_t^{G2PL,en}$) and that injected by the grid for the regulation-down offer. In (9), the total power injected from the PL to the grid (P_t^{PL2G}) is equal to the sum of that: 1) sold to the energy market ($P_t^{PL2G,en}$), 2) injected for the regulation-up offer ($P_t^{PL2G,reg,up}$), and 3) providing the reserve market offer ($P_t^{PL2G,res}$).

In (10)-(12), a condition is set such that the PL can either be injecting energy to or absorbing energy from the grid during each timeslot.

$$\mathrm{FPL2G_t} = \begin{cases} 1, & P_t^{PL2G} > 0 \\ 0, & otherwise \end{cases} \quad \forall\, t = 1 \dots NT^{PLEMS} \tag{10}$$

$$\mathrm{FG2PL_t} = \begin{cases} 1, & P_t^{G2PL} > 0 \\ 0, & otherwise \end{cases} \quad \forall\, t = 1 \dots NT^{PLEMS} \tag{11}$$

$$0 \le FPL2G_t + FG2PL_t \le 1 \quad \forall\, t = 1 \dots NT^{PLEMS} \tag{12}$$

The binary variables $\mathrm{FPL2G_t}$ and $\mathrm{FG2PL_t}$ correspond to whether power is being injected from or to the PL in timeslot t, respectively. Constraint (12) allows only one of the two to be true at the same time. With all previous definitions, the power balance constraints can be defined as shown in (13)-(15).

$$P_t^{G2PL} + P_t^{PV2PL} \le \gamma^{PL,ch} \cdot N_t^{PL} \quad \forall\, t = 1 \dots NT^{PLEMS} \tag{13}$$

$$P_t^{PL2G} \le \gamma^{PL,dis} \cdot N_t^{PL} \quad \forall\, t = 1 \dots NT^{PLEMS} \tag{14}$$

$$\Delta T^{PL} \cdot P_t^{PV2PL} \le (SOC^{PL,max} \cdot E_{t-1}^{PL,cap} - SOC_{t-1}^{PL} \cdot E_{t-1}^{PL}) - E_t^{arr} + E_t^{dep} \quad \forall\, t = 1 \dots NT^{PLEMS} \tag{15}$$

For each timeslot, the sum of the power injected from both the grid and the local PV installations to the PL (P_t^{G2PL} and P_t^{PV2PL}, respectively) must be less than or equal to the number of EVs currently stationed multiplied by the charging rate ($\gamma^{PL,ch}$).This constraints the power injected to the PL to the maximum charging capability of EVs currently stationed.

Similarly, P_t^{PL2G}must not exceed the maximum discharge capability ($\gamma^{PL,dis} \cdot N_t^{PL}$). The presence of local PV generation makes it necessary to add the third power balance constraint shown in (15). The energy charged by the PV panels is equal to the power injected (P_t^{PV2PL}) multiplied by the size of the time slot (ΔT^{PL}). The energy charged by the PV panels during any time slot must not exceed the difference between the maximum allowable energy capacity and actual energy level of the previous timeslot ($SOC_{upper} \cdot E_{t-1}^{PL,cap} - SOC_{t-1}^{PL} \cdot E_{t-1}^{PL}$), minus the energy to be added by newly arriving EVs (E_t^{arr}), plus that removed by departing ones (E_t^{dep}).

The aggregated energy stored by the PL at each timeslot can be related to the previous timeslot using (16), where $\eta_t^{PL,ch}$ and $\eta_t^{PL,dis}$ correspond to the overall charging and discharging efficiencies of the parked EVs, respectively.

$$E_t^{PL} = E_{t-1}^{PL} \tag{16}$$

$$+\Delta T \cdot \eta_t^{PL,ch}(P_t^{G2PL} + P_t^{PV2PL}) - \Delta T \cdot \frac{1}{\eta_t^{PL,dis}} \cdot (P_t^{PL2G})$$

$$\forall\, t = 1 \dots NT^{PLEMS}$$

Finding the optimal charging and discharging schedule for parked EVs involved the amount to be charged or discharged from each EV, as shown in (17) and (18), respectively. For each stationed EV at timeslot t, the SoC increment or decrement ($SOC_t^{EVID,up}$ and $SOC_t^{EVID,down}$, respectively) is defined such that the EV can only be either charging or discharging. In (19) and (20), the set of all EVs' charging and discharging schedules are compiled, respectively.

$$SOC_t^{EVID,up} = \begin{cases} 0, & \Phi_t^{EVID} = 0 \\ 0, & SOC_t^{EVID,dep} \le SOC_t^{EVID} - SOC_{t-1}^{EVID} \\ SOC_t^{EVID,dep} - SOC_t^{EVID} - SOC_{t-1}^{EVID}, & otherwise \end{cases} \quad (17)$$

$$\forall\, EVID = 1 \dots N^{EVPL}, \forall t = 1 \dots NT^{PLEMS}$$

$$SOC_t^{EVID,down} = \begin{cases} 0, & \Phi_t^{EVID} = 0 \\ 0, & SOC_t^{EVID} - SOC_{t-1}^{EVID} \le SOC_t^{EVID,dep} \\ SOC_t^{EVID,dep} - SOC_t^{EVID} - SOC_{t-1}^{EVID}, & otherwise \end{cases} \quad (18)$$

$$\forall\, EVID = 1 \dots N^{EVPL}, \forall\, t = 1 \dots NT^{PLEMS}$$

$$SOC_t^{up} = \left\{SOC_t^{1,up}, SOC_t^{2,up}, \dots, SOC_t^{N^{EVPL},up}\right\} \quad (19)$$

$$SOC_t^{down} = \left\{SOC_t^{1,down}, SOC_t^{2,down}, \dots, SOC_t^{N^{EVPL},down}\right\} \quad (20)$$

The MILP model for the PLEMS is now fully constrained. Additional constraints such as the active and reactive power flows (power factor limits) and voltage limits are added according to the grid requirements [17].

To maximize the EVPL's profit, incomes and costs must first be defined. Those are listed and described in detail in Table 1. Accordingly, the objective function ($Profit^{EVPL}$) is presented in (21), and the decision vector (**XPL**) is defined in (22)-(23).

$$\max_{\mathbf{XPL}}(Profit^{EVPL}) = \max_{\mathbf{XPL}} \sum_{t=1}^{NT^{PLEMS}} (\mathrm{IN1_t} + \mathrm{IN2_t} + \mathrm{IN3_t} + \mathrm{IN4_t} + \mathrm{IN5_t} + \mathrm{IN6_t} - \mathrm{C1_t} - \mathrm{C2_t} - \mathrm{C3_t} - \mathrm{C4_t} - \mathrm{C5_t} - \mathrm{C6_t} - \mathrm{C7_t} - \mathrm{C8_t}) \quad (21)$$

$$\mathbf{XPL} = \left\{\boldsymbol{XPL_1}, \boldsymbol{XPL_2}, \dots, \boldsymbol{XPL}_{NT^{PLEMS}}\right\} \quad (22)$$

$$\boldsymbol{XPL_t} = \{SOC_t^{up}, SOC_t^{down}, P_t^{PV2PL}, P_t^{G2PL,en}, P_t^{PL2G,en}, P_t^{G2PL,reg,down}, P_t^{PL2G,reg,up}, P_t^{PL2G,res}\} \quad (23)$$

Table 1. Detailed description of the profit and cost terms used for the PLEMS. Unit prices are based on the electricity market being considered [17].

Term	Description	Unit Price
Income: $IN1_t$	Energy sold to grid as active power injection from the PL ($P_t^{PL2G,en}$).	λ_t^{en} €/kWh
Income: $IN2_t$	Energy sold for the ISO-requested reserve ($P_t^{PL2G,res}$).	λ_t^{res} €/kWh
Income: $IN3_t$	Tariff paid by EV owners for energy charged to their EVs ($P_t^{G2PL} + P_t^{PV2PL}$).	$\lambda_t^{EV,ch}$ €/kWh
Income: $IN4_t$	Hourly tariff paid by EV owners for to park in the PL ($P_t^{G2PL} + P_t^{PV2PL}$).	$\lambda_t^{EV,park}$ €/h
Income: $IN5_t$	Energy exchanged for the ISO-requested regulation-up ($P_t^{PL2G,reg,up}$).	$\lambda_t^{reg,up}$ €/kWh
Income: $IN6_t$	Energy exchanged for the ISO-requested regulation-down ($P_t^{PL2G,reg,down}$).	$\lambda_t^{reg,down}$ €/kWh
Cost: $C1_t$	Energy purchased from the grid as active power injection to the PL ($P_t^{G2PL,en}$).	λ_t^{en} €/kWh
Cost: $C2_t$	Tariff paid to EV owners for energy discharged from their EVs.	$\lambda_t^{EV,dis}$ €/kWh
Cost: $C3_t$	Compensation paid to EV owners for battery degradation by V2G in energy market.	Cd^{en} €/kWh
Cost: $C4_t$	Compensation paid to EV owners for battery degradation by V2G in reserve market.	Cd^{en} €/kWh
Cost: $C5_t$	Compensation paid to EV owners for battery degradation by V2G in regulation market.	Cd^{reg} €/kWh
Cost: $C6_t$	Penalty paid for failing to provide the ISO-requested reserve ($P_t^{PL2G,res}$).	$0.02 \cdot \lambda_t^{res}$ €/kWh
Cost: $C7_t$	Penalty paid for failing to deliver the ISO-requested regulation-up ($P_t^{PL2G,reg,up}$).	$0.02 \cdot \lambda_t^{reg,up}$ €/kWh
Cost: $C8_t$	Penalty paid for failing to deliver the ISO-requested regulation-down ($P_t^{PL2G,reg,down}$).	$0.02 \cdot \lambda_t^{reg,down}$ €/kWh

2.3 Home Energy Management System

In this study, the HEMS models a smart home incorporating an EV, local PV generation, dynamic DR tariffs, and shiftable loads. By considering the homeowner's preferences for the usage time of each shiftable load, MILP optimization is used to obtain the day-ahead schedule that minimizes the electricity bill. The mathematical formulation of the model is presented in this section.

With residential DR participation, the final electricity bill is the difference between energy bought from the grid and energy sold back. The objective function (Z), to be minimized, is defined in (24): The total power injected from the grid to the home (bought) for each timeslot *t* is represented as P_t^{G2H} at a unit price of λ_t^{buy}. In this model, the energy stored by the ESS is used directly for self-consumption never injected into the grid. Therefore, P_t^{H2G} (total power sold to the grid at a unit price λ_t^{sell}) is equal to excess PV generation. Similar to the PLEMS, the HEMS day-ahead time discretization is shown in (25), Such that scheduling is performed for each timeslot $t = 1 \dots NT^{HEMS}$, and the duration of each timeslot is ΔT^{HEMS}.

$$\min Z = \min \sum_{t=1}^{NT^{HEMS}} \Delta T^{HEMS} \left(P_t^{G2H} \lambda_t^{buy} - P_t^{H2G} \lambda_t^{sell} \right) \tag{24}$$

$$\Delta T^{HEMS} = \frac{24}{NT^{HEMS}} \tag{25}$$

Two stages are defined: 1) before HEMS implementation, which are the baseline operation intervals based on the end-user preferences; and 2) after HEMS implementation, where the flexible loads are optimally scheduled based on the DR tariffs.

The initial stage (before HEMS implementation) is first modeled by defining the operating intervals of each load i from a total number of N^{shift} shiftable loads. This is defined as the baseline interval for each load i as shown in (25), with $LB_{i,b}$ and $UB_{i,b}$ being the baseline lower and upper bounds, respectively. The binary variable $B_{i,t}$ is set to 1 during the timeslots t when the load i is operating and 0 for all timeslots outside its operating interval.

$$B_{i,t} = \begin{cases} 0 & t < LB_{i,b} \\ 1 & LB_{i,b} \le t \le UB_{i,b} \\ 0 & t > UB_{i,b} \end{cases} \quad \forall\, t = 1 \dots NT^{HEMS} \tag{26}$$

In the second stage (HEMS implementation), flexible loads are shifted from the baseline intervals to reduce costs according to dynamic DR tariffs (i.e., shifting from peak to off-peak periods). However, not all loads are indefinitely shiftable and so users set allowable lower and upper intervals for each load to operate, represented as $LB_{i,u}$ and $UB_{i,u}$, respectively. The output of the HEMS would include the new scheduled slots for each load as shown in (27). The binary variable $S_{i,t}$ corresponds to the timeslots that the load i is scheduled to operate by the HEMS, in the interval between $LB_{i,s}$ and $UB_{i,s}$. The scheduled operating interval must lie within the limits set by the user, as set by constraints (28) and (29).

$$S_{i,t} = \begin{cases} 0 & t < LB_{i,s} \\ 1 & LB_{i,s} \le t \le UB_{i,s} \\ 0 & t > UB_{i,s} \end{cases} \quad \forall\, t = 1 \dots NT^{HEMS} \tag{27}$$

$$LB_{i,s} \ge LB_{i,u}\,, \qquad \forall i = 1, \dots, N^{shift} \tag{28}$$

$$UB_{i,s} \le UB_{i,u}\,, \qquad \forall i = 1, \dots, N^{shift} \tag{29}$$

Moreover, (30) indicates that while the scheduled of each shiftable load is shifted, the operating duration is unchanged.

$$\sum_{t=1}^{NT^{HEMS}} S_{i,t} = \sum_{t=1}^{NT^{HEMS}} B_{i,t}\,, \qquad \forall i = 1, \dots, N^{shift} \tag{30}$$

The total day-ahead energy demand of the house (E^{HD}) is shown in (31) and is the sum of two terms: the energy demand of scheduled loads and the base load (P_t^{HBase}). Due to the constraint by (30), the total energy demand before and after scheduling is unchanged. The power demand for each timeslot (P_t^{HD}) is expressed in (32).

$$E^{HD} = \sum_{i=1}^{N^{shift}} \sum_{t=1}^{NT^{HEMS}} \left(\frac{S_{i,t} \cdot P_i}{\Delta T^{HEMS}}\right) + \sum_{t}^{NT} \frac{P_t^{HBase}}{\Delta T^{HEMS}} \tag{31}$$

$$P_t^{HD} = \sum_{i=1}^{N^{shift}} \left(S_{i,t} \cdot P_i \right) + P_t^{HBase} \tag{32}$$

The model considers the presence of an ESS and local PV generation. For the ESS, constraints (33)-(38) are applied. Binary variables $\mathrm{ESSCH_t}$ and $\mathrm{ESSDIS_t}$; indicate whether the ESS is charging or discharging during timeslot t, respectively. The ESS can only be either charging or discharging in a given timeslot as indicated by (33).

In (34) and (35), the charging and discharging power ($P_t^{HESS,ch}$ and $P_t^{HESS,dis}$, respectively) of the ESS are limited by maximum charging and discharging rate ($\gamma^{HESS,ch}$ and $\gamma^{HESS,dis}$), respectively. In (36), the energy stored by the ESS is updated for timeslot *t*, considering that of the previous timeslot and charged/discharged energy. The SoC, shown in (37) as the ratio of current energy stored to the rated capacity ($E_t^{HESS,Cap}$), is constrained by the minimum and maximum allowable limits in (38). While the EV charging is considered a shiftable load to be scheduled by the HEMS, the technical constraints (33)-(38) apply to the EV battery when it is parked at home.

$$0 \leq \mathrm{ESSCH_t} + \mathrm{ESSDIS_t} \leq 1, \qquad \forall t = 1 \dots NT^{HEMS} \tag{33}$$

$$P_t^{HESS,ch} \leq \mathrm{ESSCH_t} \cdot \gamma^{HESS,ch}, \qquad \forall t = 1 \dots NT^{HEMS} \tag{34}$$

$$P_t^{HESS,dis} \leq \mathrm{ESSDIS_t} \cdot \gamma^{HESS,dis}, \qquad \forall t = 1 \dots NT^{HEMS} \tag{35}$$

$$E_t^{HESS} = E_{t-1}^{HESS} + \eta^{HESS,ch} \cdot \Delta T^{HEMS} \cdot P_t^{HESS,ch} - \frac{1}{\eta^{HESS,dis}} \cdot \Delta T^{HEMS} \cdot P_t^{HESS,dis} \qquad \forall t = 1 \dots NT^{HEMS} \tag{36}$$

$$SOC_t^{HESS} = \frac{E_t^{HESS}}{E^{HESS,Cap}}, \qquad \forall t = 1 \dots NT^{HEMS} \tag{37}$$

$$SOC^{HESS,min} \leq SOC_t^{HESS} \leq SOC^{HESS,max}, \qquad \forall t = 1 \dots NT^{HEMS} \tag{38}$$

The net power generated by the home PV panels (P_t^{HPV}) in a given timeslot must either be self-consumed (P_t^{HPV2H}) or sold to the grid (P_t^{HPV2G}) as indicated by (39).

$$P_t^{HPV} = P_t^{HPV2H} + P_t^{HPV2G}, \qquad \forall t = 1 \dots NT^{HEMS} \tag{39}$$

The final constraint for the HEMS is the power balance constraint, which is shown in (40) for each timeslot *t*.

$$P_t^{HPV2H} + P_t^{G2H} = P_t^{HD} + P_t^{HESS,ch} - P_t^{HESS,dis} + P_t^{HPV2G} \qquad \forall t = 1 \dots NT^{HEMS} \tag{40}$$

2.4 Coordinating the Energy Management Systems

The primary link between the individual EMSs are the EVs. In (41) and (42), the arrival/departure times to/from the home and PL are related using TCOM (commuting time) for each EV. Given the arrival and departure time from only one of the two locations, accurate commuting times can be obtained by means of online cloud applications such as map and navigation services, which account for real traffic data. Thus, the EV owner can only provide the departure time from home and departure time from the PL, and the other times can be automatically computed. Similarly, the SoC of the EV battery at the destination is equal to that upon departure from the source minus the SoC lost during the commute, as in (43) and (44).

$$t^{EVID,arr,PL} = t^{EVID,dep,H} + TCOM^{EVID,2PL}, \forall EVID \quad (41)$$

$$t^{EVID,arr,H} = t^{EVID,dep,PL} + TCOM^{EVID,2H}, \forall EVID \quad (42)$$

$$SOC^{EVID,arr,PL} = SOC^{EVID,dep,H} - \Delta\mathrm{SOC}^{EVID,2PL}, \forall EVID \quad (43)$$

$$SOC^{EVID,arr,H} = SOC^{EVID,dep,PL} - \Delta\mathrm{SOC}^{EVID,2H}, \forall EVID \quad (44)$$

The SoC lost during the commute ($\Delta\mathrm{SOC}$) can be calculated based on the commute distance (DCOM) and average driving efficiency of the EV model ($\eta^{drive,}$ %/km), as in (45) and (46).

$$\Delta\mathrm{SOC}^{EVID,2PL} = DCOM^{EVID,2PL} \cdot \eta^{drive,EVID}, \forall EVID \quad (45)$$

$$\Delta\mathrm{SOC}^{EVID,2H} = DCOM^{EVID,2H} \cdot \eta^{drive,EVID}, \forall EVID \quad (46)$$

Using (41)-(46), it is possible to coordinate the operation of the PLEMS and individual HEMSs without needing to share private information by either side. The HEMS only needs to share the EV arrival time at PL, EV departure time from PL, and arrival SoC. Meanwhile, the PLEMS shares each EV's departure SoC with its HEMS. Any extra information needed by the EMSs (e.g., PV forecasts, electricity market data, traffic data, etc.) is obtained through public cloud/web applications and repositories. The interaction and information flow between the EMSs and different elements is illustrated in Fig. 3.

The developed and presented EMSs, along with the proposed coordination framework, are robust and adaptable to any decision-making timeframe or time resolution. However, the only requirement with regards to when the information should be shared is posed by the nature of day-ahead electricity markets. This of course does not preclude from the fact that updating the schedules via frequent information exchange can take place especially when high levels of uncertainty are foreseen.

Nonetheless, in real-life applications, an exchange of information must always take place at the closure of the day-ahead market (i.e., 12 AM in most cases) regardless of the decision-making horizon and/or time resolutions used by the individual EMSs.

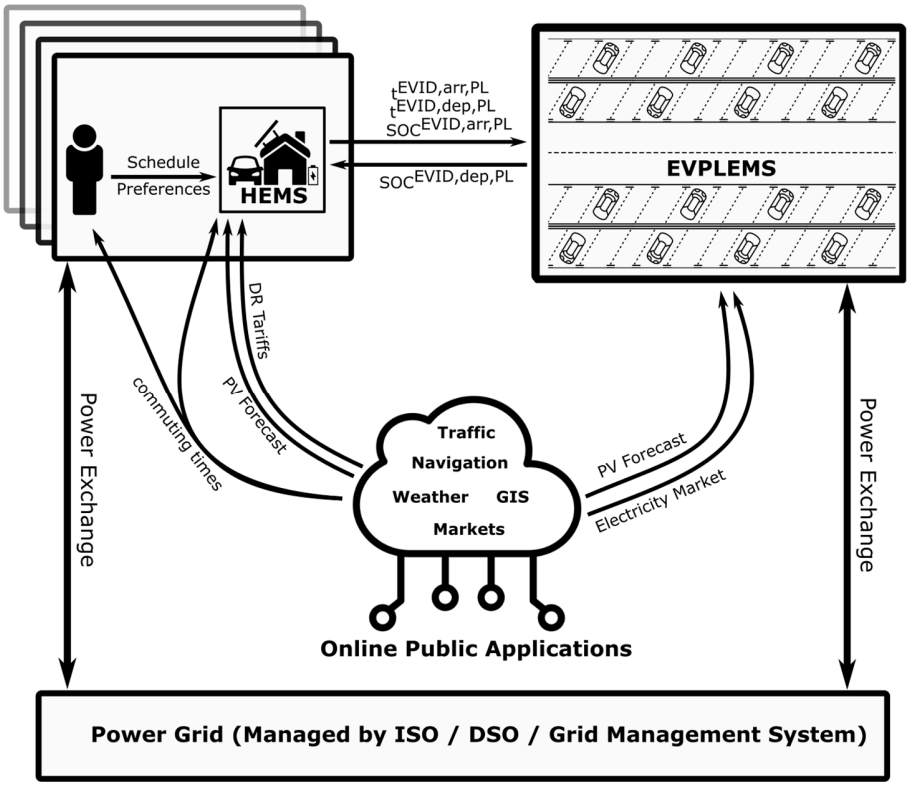

Fig. 3. An illustration of the interactions and information flow between the PLEMS, HEMSs, cloud/web public services and repositories, and the power grid in the considered scheme.

3. Case Study

To simulate the proposed scheme, a case study based on real-world conditions was designed. By computationally simulating the four scenarios described in Section II.A, possible synergies (or drawbacks) resulting from the interaction between the EMSs can be observed and evaluated.

The modeled EVPL was based on one of the parking spaces of the Faculty of Engineering of University of Porto (FEUP). This EVPL, along with variations of it, has been previously used in [16] to test the PLEMS system. It is assumed that a total of 108 EVs are enlisted in this EVPL (students and staff members). The EVPL has PV panels installed with a rated output power of 100 kW [18]. As a common EV model in Portugal, the Nissan Leaf, with a 30kWh battery was used to model all EVs. The full specifications of the Nissan Leaf can be found in [7].

The smart homes corresponding to each of the 108 EVs have local PV installations with a 3kW rated output power and the LG RESU 6.5kWh lithium-ion ESS. The complete specifications of the home PV panels and ESS can be found in [19] and [9], respectively. The homes are in one of two neighborhoods located in different places of the metropolitan area of Porto. In this way, the effect of different commuting times can be compared. Neighborhoods 1 and 2 have 72 and 36 homes, respectively (total of all 108 homes).

The average SoC lost when commuting between the EVPL and each of the neighborhoods is shown in Table 2. In this table, the variation of the SoC lost (accounting for traffic conditions) is represented as a standard deviation from the mean value. Given the nature of study and work times at the faculty, some EV owners have a morning schedule, while others have an afternoon schedule.

On average, the ones with morning schedules arrive at the EVPL at 9:00 and leave by 18:00, while the ones with an afternoon schedule arrive at 14:00 and leave by 21:00. Variations in the individual arrival and departure times of individual EV owners were considered, with the arrival and departure times varying from the average ones as show in Table 3. The "Max" value represents the latest possible arrival time (11:30 for the morning and 16:30 for the afternoon).

By accounting for the uncertainties in both the commuting times and commuting time and the arrival/departure times, real-life conditions are captured. A code script was made to generate individual arrival/departure times and transit times for each EV, for each day simulated. An example schedule for a given day using the is shown in Fig. 4. By generating the arrival/departure schedules to/from the homes and the EVPL, the proposed coordination framework between the EMSs can be tested and validated.

Table 2. Average SoC lost in commute, assumed variations due to traffic uncertainties (based on a normal distribution), and the breakdown of morning and afternoon EVs in each neighborhood.

Location	Mean SoC Lost in Commute to/from EVPL	Variation with Traffic (as std. deviation)	Total Number of Homes (and EVs)	Number of Morning Schedule EVs	Number of Afternoon Schedule EVs
Neighborhood 1	0.2	0.02	72	48	24
Neighborhood 2	0.3	0.03	36	24	12

Table 3. Morning and afternoon schedules and uncertain variations in the arrival and departure times, based on a normal distribution.

Work Schedule		Mean	Std. Deviation	Max
Morning	Arrival Time	9:00	50 min	11:30
	Departure Time	18:00		-
Afternoon	Arrival Time	14:00	50 min	16:30
	Departure Time	21:00		-

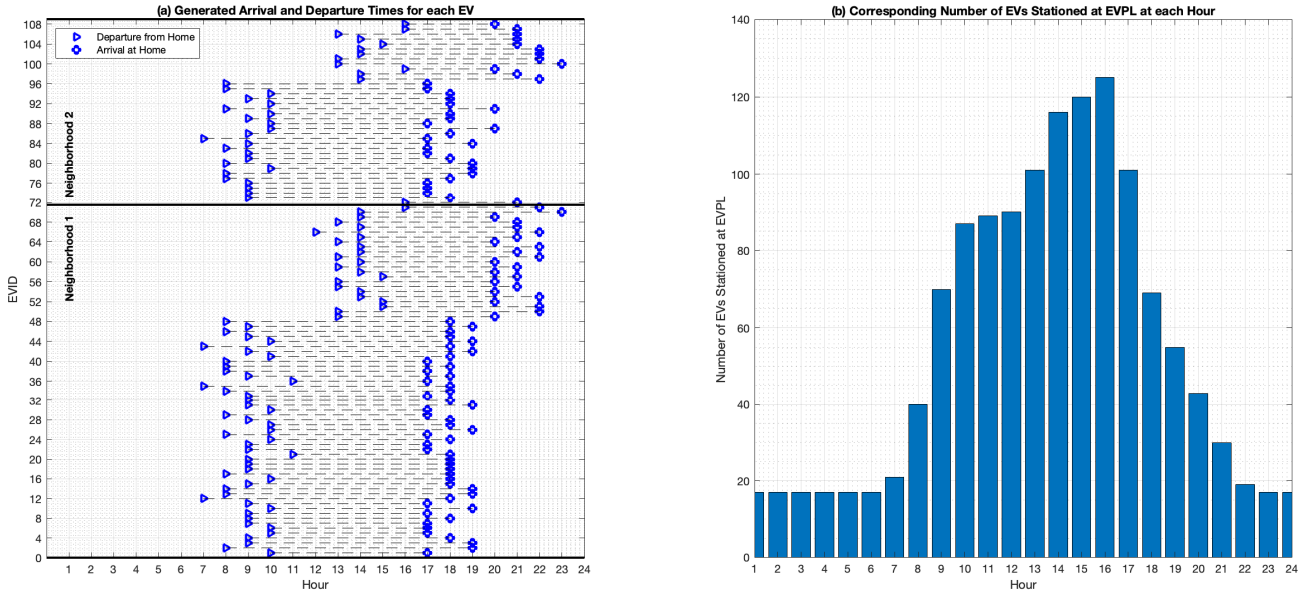

Fig. 4. An example schedule of all EVs for a given day using the scheduling script showing (a) the arrival and departure times from home and (b) the corresponding number of EVs stationed at the EVPL at each hour. For every new day being simulated, a new schedule is generated considering uncertainties of arrival/departure and commuting times based on Table 2 and Table 3.

Finally, the power grid is simulated using the IEEE 33-bus test system, a standard radial test system operating at 12.66 kV line voltage [20]. The locations of the EVPL and the neighborhoods both on the map and on the power grid are illustrated in Fig. 5. The generator costs and bus loads are modified according to the real electricity market data to be considered in each case study.

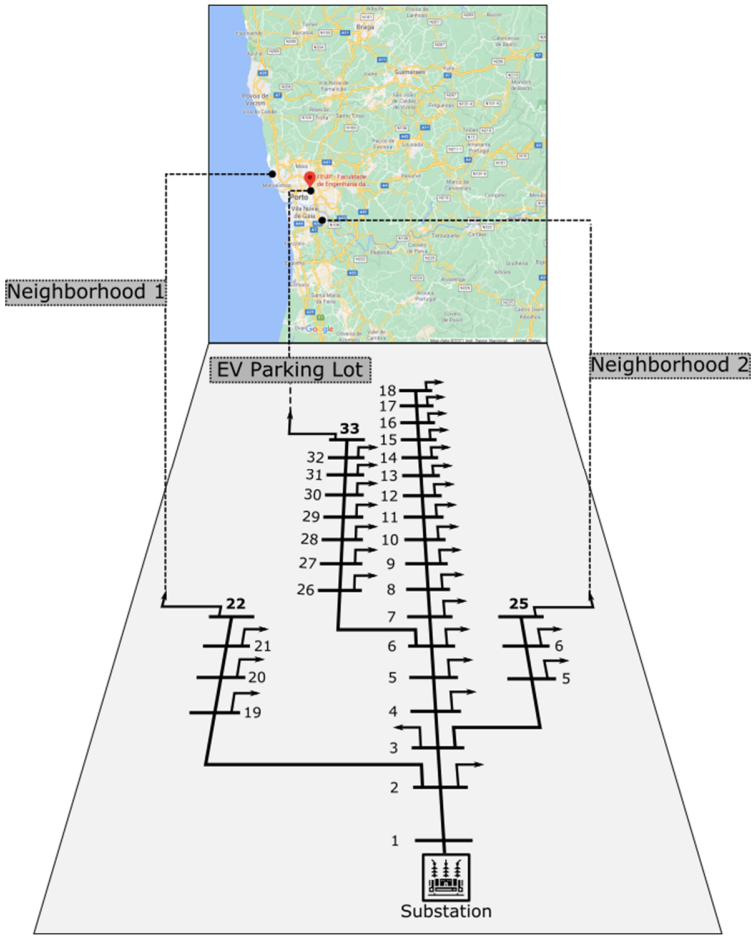

Fig. 5. The map location of the EVPL and two neighborhoods used in the case study, and the corresponding buses on the IEEE 33-bus standard test system [20].

Neighborhoods 1 and 2 are connected to buses 22 and 25, respectively, and the EVPL to bus 33. Typical low voltage commercial and residential load profiles publicly available by the Portuguese Energy Regulation Services Entity (ERSE) [21], BTN and BTE (1 and 2), respectively, were used for the other buses as shown in Table 4. In this manner the hourly loads at the buses in the test system would reflect the electricity market data. As such, the generator costs are set to the real day-ahead market prices of the day under study (in this paper the Iberian market, and only energy and regulation markets were considered). The bus loads are set according to the ERSE typical load profiles of the same day. The power exchange at buses 22, 25, and 33 is according to the EMSs output. For each case study considered in the next section the considered days and corresponding market and load conditions are specified. All other parameters assumed for the PLEMS and HEMS are according to those in [18], [19]. Accordingly, one day of operation is simulated using the following steps:

Step 1: Generate individual schedules - arrival/departure times and transit times for each EV.

Step 2: Run PLEMS code to determine departure SoC of each EV, and power exchange with the grid at bus 33.

Step 3: Run HEMS code for each individual home to determine power exchange with the grid at buses 22 and 25.

Step 4: At each timestep, run AC optimal power simulation for the power grid.

Table 4. Loads connected to the simulated power grid. BTN, BTE1, and BTE2 daily typical load profiles are publicly available online by ERSE [21].

Bus	Load	Bus	Load	Bus	Load
1	**Slack Bus**	**12**	*Commercial - BTN*	**23**	*Residential – BTE1*
2	*Commercial - BTN*	**13**	*Commercial - BTN*	**24**	*Residential – BTE1*
3	*Commercial - BTN*	**14**	*Commercial - BTN*	**25**	***Neighborhood 2***
4	*Commercial - BTN*	**15**	*Commercial - BTN*	**26**	*Residential – BTE2*
5	*Commercial - BTN*	**16**	*Commercial - BTN*	**27**	*Residential – BTE2*
6	*Commercial - BTN*	**17**	*Commercial - BTN*	**28**	*Residential – BTE2*
7	*Commercial - BTN*	**18**	*Commercial - BTN*	**29**	*Residential – BTE2*
8	*Commercial - BTN*	**19**	*Residential – BTE1*	**30**	*Residential – BTE2*
9	*Commercial - BTN*	**20**	*Residential – BTE1*	**31**	*Residential – BTE2*
10	*Commercial - BTN*	**21**	*Residential – BTE1*	**32**	*Residential – BTE2*
11	*Commercial - BTN*	**22**	***Neighborhood 1***	**33**	***EVPL***

4. Simulations and Results

In this section, the results of the simulations are shown and discussed. Two separate studies were performed. The first is done from the technical perspective, where the objective is to analyze the effect of the EMSs coordination on the power flow in the grid. The second analysis is performed from an economic perspective, illustrating the point of view of the EV owners to analyze the cost-efficiency of the proposed EMS coordination scheme. All simulations were run on a standard laptop computer with an Intel Corei7-8550U CPU @ 1.80 GHz, 16.0 GB RAM, and a Windows 10 64 bit operating system. The General Algebraic Modelling System (GAMS) environment was used to implement the PLEMS and HEMS, applying the Mixed Integer Programming (MIP) solver. MATPOWER 7.1 on MATLAB 2019b was used for the power flow simulations.

4.1 Technical Viability: Power Flow Analysis

To incorporate effects of seasonal variations, two working days were analyzed: a winter day (21-Jan-2019) and a summer day (01-Jul-2019), both a Monday for consistency. As mentioned, the 33-bus test system is modified by applying the ERSE load profiles to the bus loads. By doing so, the system peak load is 3.05 MW and 2.94 MW for the winter and summer days, respectively.

For the homeowners, the summer and winter residential tariffs are shown in Fig. 5, according to commercial tri-hourly electricity tariffs in Portugal, which can be seen found in [22]. For the EVPL, the energy and regulation market prices are according to the Iberian market, which are available online by the Portuguese TSO (REN) [23]. The energy price in the Iberian market is also plotted in Fig. 6. It is assumed that both the PL and homes use maximum power point tracking (MPPT) PV installations, and it is also assumed the normalized (unit) MPPT generation is the same for both. All generator costs are set in accordance with the energy price for the given hour/day. In this manner, for a given day being simulated, all real market conditions are used.

Accordingly, real PV generation data was obtained from a smart home [18] in Porto for the given days and the normalized MPPT generation is shown in Fig. 7. After generating the daily arrival/departure and commuting schedules for all 108 EVs, the aggregated load profiles of Neighborhood 1 and 2 are shown in Fig. 8. The HEMS settings and preferences are provided in Appendix 1 and the HEMS operation for a single home is demonstrated in Appendix 2. It is noteworthy that no two homes have the same profile, due to the variations of the individual schedule for each home. The energy exchanged between the grid and each of the EMSs installed is shown for the neighborhoods and the PL in Fig. 9 and 10, respectively.

In Fig. 11, active power losses are plotted for all four scenarios. As mentioned in Section 2.1, evaluating these intermediate scenarios can provide some insight of the contribution of each EMS to the final result. In Figs. 12 and 13, scenarios 1 (base) and 4 (final) are compared for all variables of interest (voltages at buses 22, 25, and 33, total power supplied by grid, and total power losses) between the summer and winter cases.

In Fig. 11 it is observed that applying only the HEMSs has a slight but consistently favorable effect on grid losses. This is expected, since the HEMS favors self-consumption and only injects to the grid in times of excess PV generation, which is also a time of high load demand.

By looking at Fig. 12(c)-(d) and 13(c)-(d), it can be seen that very minimal (barely observable) change occurs in the voltage profiles at the neighborhoods buses. With or without EMSs, the p.u. voltage at the neighborhood buses is very close to 1 for both the winter and summer days. Meanwhile, the PLEMS can be seen to have a more significant impact on the power flow results. The average and peak deviations between S4 and S1 were extracted and detailed in Table 6.

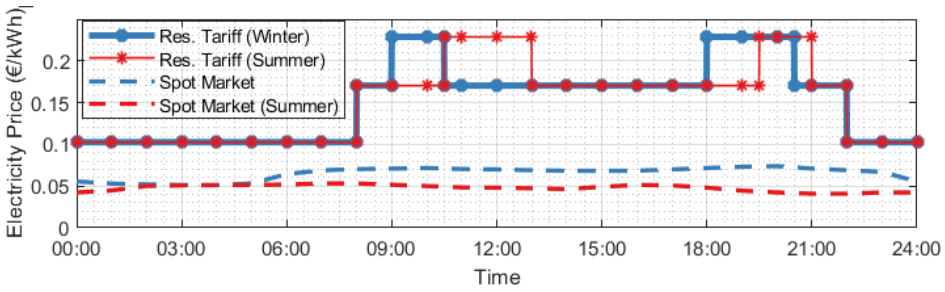

Fig. 6. Residential tariffs and Iberian market prices for summer and winter days.

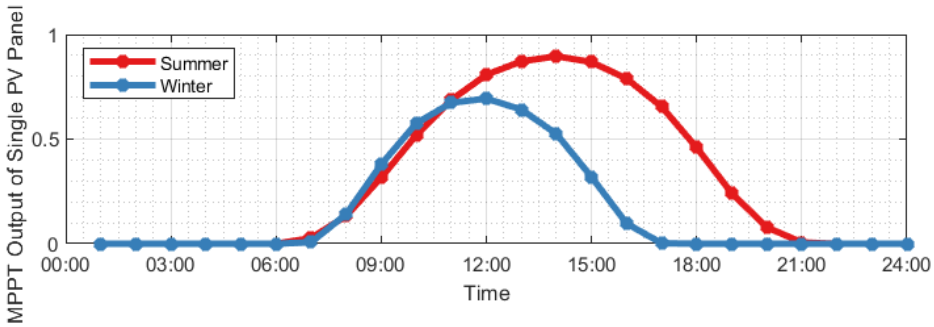

Fig. 7. Normalized MPPT PV output for the summer and winter days.

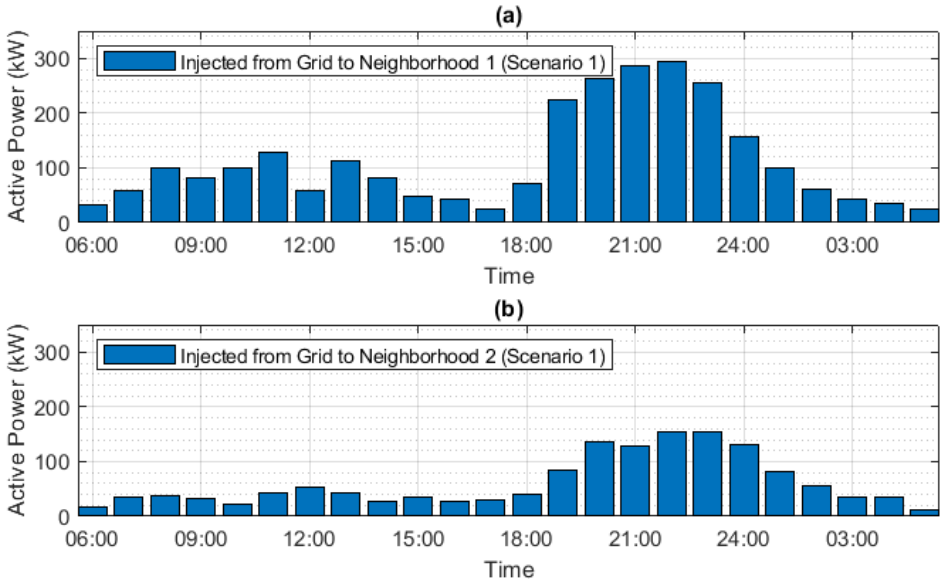

Fig. 8. Active power load profile with no EMSs (scenario 1) in the summer day for a) Neighborhood 1 and b) Neighborhood 2.

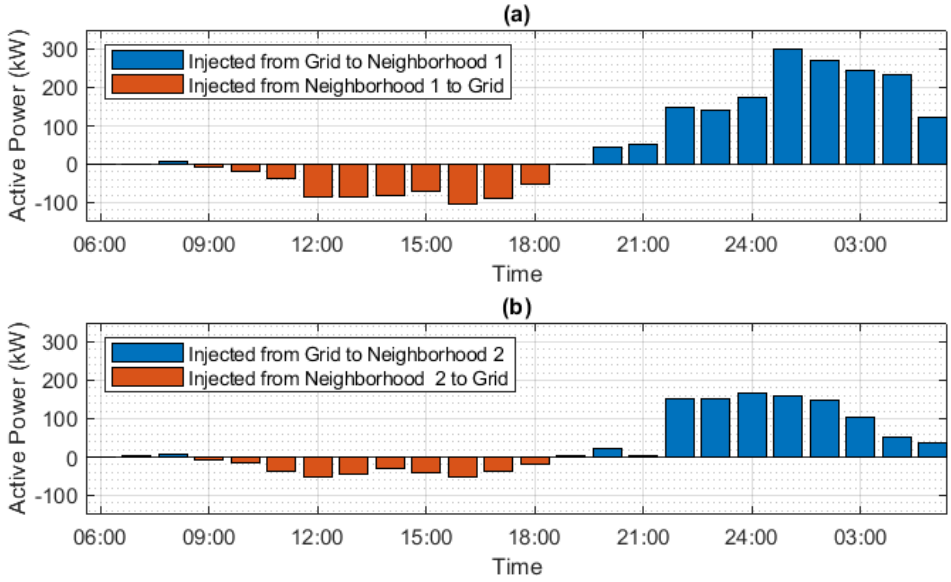

Fig. 9. Active power exchanged with grid with coordinated EMSs (scenario 4) in the summer day for (a) Neighborhood 1 and (b) Neighborhood 2.

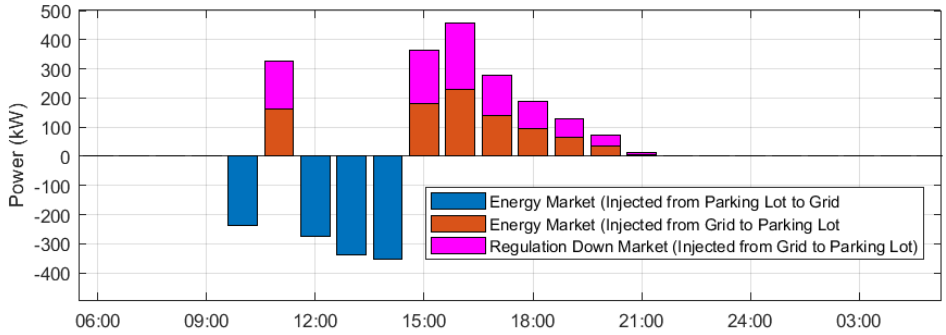

Fig. 10. Active power exchanged with grid with coordinated EMSs (scenario 4) in the summer day for the EVPL, due to participation in the energy and regulation markets.

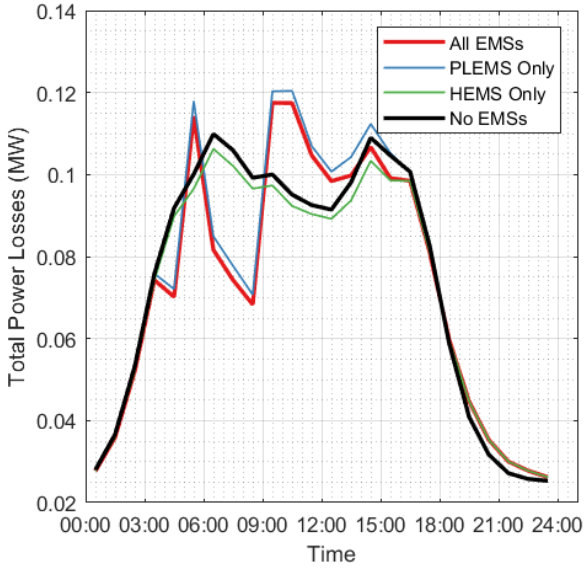

Fig. 11. Comparison of active power losses for all scenarios (summer).

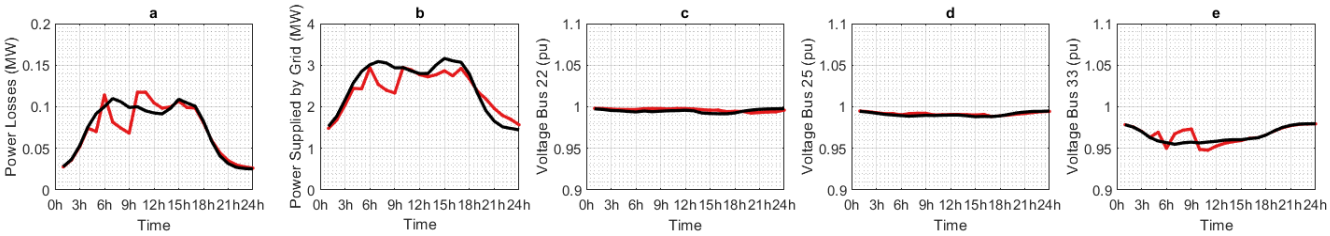

Fig. 12. Power flow results for the summer day: (a) grid active power losses, (b) active power supplied by the grid, (c) voltage at Neighborhood 1, bus 22 (d) voltage at Neighborhood 2, bus 25, and (e) voltage at EVPL, bus 33. Black line represents base scenario (no EMSs) red line represents final scenario (all EMSs).

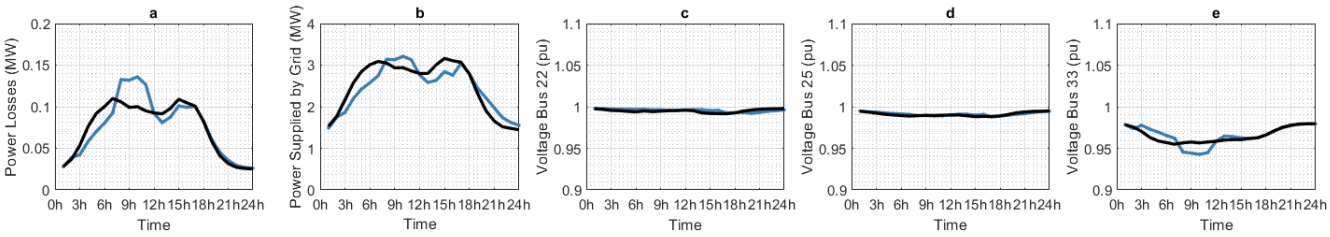

Fig. 13. Power flow results for the winter day: (a) grid active power losses, (b) active power supplied by the grid, (c) voltage at Neighborhood 1, bus 22 (d) voltage at Neighborhood 2, bus 25, and (e) voltage at EVPL, bus 33. Black line represents base scenario (no EMSs) red line represents final scenario (all EMSs).

From Fig. 11 it can be seen that the intermediate scenario 3 (with the PLEMS and without the HEMSs) is very similar to the final scenario 4 (with all EMSs). In scenario 3, during the summer day the power losses are dramatically decreased in the morning (at 09:00). In this time the majority of EVs are arriving to the PL and are available to operate in V2G modes, and PV generation starts. With both factors combined, the EVPL starts to inject power to the grid and this is met with the observed drop both in power losses and power supplied by the grid.

In Fig. 12(d) it can be seen that this corresponds to an observable over-voltage due to the injected power to the grid. In the winter, the exact opposite occurs at this time, since the morning surge of EVs occurs when PV generation is not enough and an undervoltage occurs since power has to be consumed from the grid.

Around 12:00, the opposite occurs. The PL is full at this time and requires energy from the grid to charge the parked EVs (as seen in Fig. 10). However, due to PV generation and self-consumption, this is still met with a decrease in system losses and power supplied by the grid; and an undervoltage can be observed. Since this is around the peak PV generation time, the same effect is observed in the winter albeit with less magnitude.

The total power loss and power supplied by the grid for both days are reported in Table 6, This effect results in the observed shift of the peak power losses time of the day. From this study, the following inferences can be drawn:

- A synergistic effect is observed in which an added benefit is obtained by applying all the EMSs compared to each one separately.
- Overall, all observed power flow variables show added benefits for the summer day compared to the winter one.
- The employed HEMSs have a slight but consistently favorable effect on the power grid.
- The employed PLEMS has a more significant effect on the power grid. During the summer the morning surge results in a drop in grid power losses and an overvoltage at the PL bus. During the winter, the morning surge causes a significant undervoltage due to insufficient PV generation.
- The employed PLEMS has a more significant effect on the power grid. During the summer the morning surge results in a drop in grid power losses and an overvoltage at the PL bus. During the winter, the morning surge causes a significant undervoltage due to insufficient PV generation.
- All voltages in the network, for all cases, are well within the allowed safety range (0.9-1.1).

Table 5. Results from the power flow analysis: comparison of average and peak deviations (winter and summer) between the optimized S4 scenario vs. the baseline S1 scenario, for active power losses, active power provided by the grid, and voltages.

	Avg. Deviation (S4 vs. S1)		Peak Deviation (+ve) (S4 vs. S1)		Peak Deviation (-ve) (S4 vs. S1)	
	Summer	Winter	Summer	Winter	Summer	Winter
Grid Total Active Power Losses	- 0.33 %	+ 1.44 %	+ 23.49 % at 11:00	+35.85 % at 10:00	- 31.16 % at 9:00	-23.62 % at 5:00
Active Power Injection by Grid	- 2.49 %	- 0.66 %	+ 18.40 % at 21:00	+ 19.16 % at 21:00	- 21.45 % at 8:00	-14.81 % at 5:00
Voltage @ Neighborhood 1, Bus 22	+ 0.001 pu	< 0.001 pu	+ 0.004 pu at 16:00	+ 0.004 pu at 16:00	- 0.004 pu at 21:00	- 0.004 pu at 20:00
Voltage @ Neighborhood 2, Bus 25	< 0.001 pu	< 0.001 pu	+ 0.003 pu at 8:00	+ 0.002 pu at 16:00	- 0.002 pu at 21:00	- 0.002 pu at 21:00
Voltage @ EVPL, Bus 33	< 0.001 pu	< 0.001 pu	+ 0.016 pu at 9:00	+0.011 at 5:00	- 0.010 pu at 11:00	- 0.014 pu at 10:00

Table 6. Results from the power flow analysis: total energy supplied and total energy losses comparison between S1 and S4, for the winter and summer.

Season	Winter		Summer	
Scenario	No EMSs (S1)	All EMSs (S4)	No EMSs (S1)	All EMSs (S4)
Total Energy Supplied (MWh)	59.8	58.6	59.8	57.2
Total Energy Losses (MWh)	1.8	1.8	1.8	1.7

4.2 Economic Viability: Cost Analysis for EV Owners

With the technical viability of the proposed scheme confirmed, a second study was performed to analyze the economic aspect from the EV owners' point of view. As it is advised to investigate the worst-case scenario for economic purposes, the winter case was used. The simulations were extended for the entire week, rather than one day, for the working week corresponding to 21/25-Jan-2019. A single EV was extracted and analyzed to obtain the total electricity costs for the full working week. The results of this study are shown in Fig. 12 (a)-(d), and Tables 5 and 6. By tracking the full SoC variation during the working week, the total electricity bill for the EV owner can be calculated based on the: i) cost of purchasing electricity at home, ii) profit from selling energy to grid at home, iii) tariffs paid to the PL for parking and charging, iv) income from the parking lot for V2G compensation.

The breakdown of the week electricity bill for the EV under study is shown in Table 7.

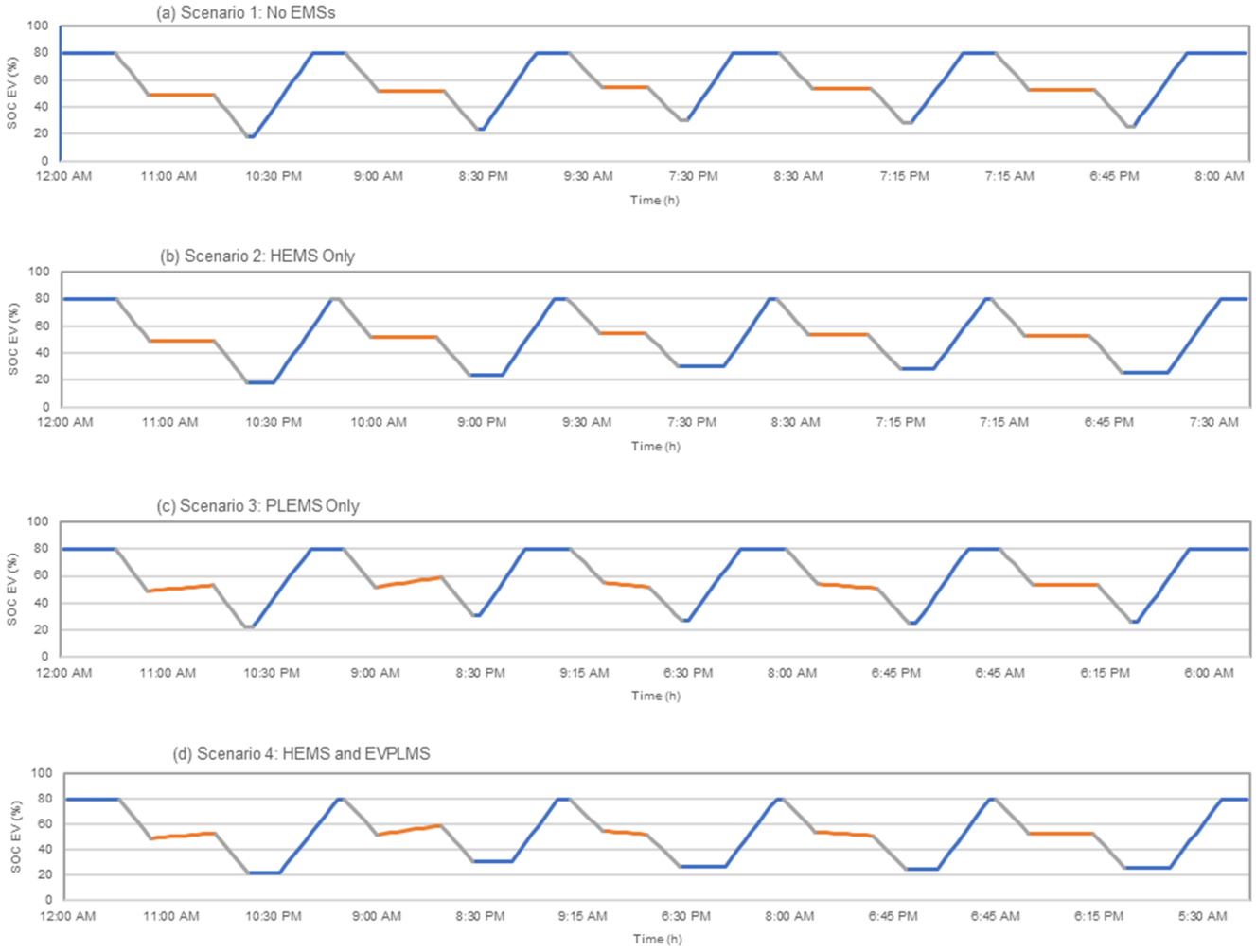

Fig. 13. SoC variation during the full winter working week for the EV under study in the case of (a) S1 - no EMSs, (b) S2 - only HEMSs, (c) S3 - PLEMS only, (d) S4 - all EMSs. Blue, orange, and gray segments correspond to when the EV is at home, in transit, or at the EVPL, respectively.

Table 6. Total electricity bill of the EV owner for each of the considered scenarios and the percentage gain or loss compared to the baseline scenario (S1).

Scenario	Day					Total Electricity Bill for the Working Week	Reduction (-ve) or Increase (+ve) Compared to (S1)
	1	2	3	4	5		
S1 (No EMS - Baseline)	€ 1.37	€ 1.08	€ 1.03	€ 1.11	€ 1.21	**€ 5.79**	**-**
S2 (HEMS only)	€ 1.25	€ 0.93	€ 0.81	€ 0.96	€ 1.05	**€ 4.99**	**- 14 %**
S3 (PLEMS only)	€ 1.61	€ 1.48	€ 0.87	€ 0.94	€ 1.21	**€ 6.11**	**+ 6 %**
S4 (Coordinated HEMS and PLEMS)	€ 1.46	€ 1.32	€ 0.64	€ 0.82	€ 1.05	**€ 5.30**	**- 9 %**

From the obtained results the following observations can be made:

- Employing the HEMS in S2 introduces a significant reduction in the weekly electricity bill compared to the base case(-14%).
- Employing the PLEMS alone in S3 has a negative effect on the EV owner: an increase of 6% in the total bill. This is expected since the PLEMS's objective function is to maximize the EVPL's profit.
- Employing the HEMS along with PLEMS in S4 overcomes the adverse effect of the previous scenario and results in a net reduction in the bill compared to the base scenario (-9%).

5. Recommendations for Future Work

Overall, the employment of the presented EMSs and the proposed coordination framework has been shown to have potential benefits, being both technically viable for the power grid and economically beneficial for the EV owners. With a certain progression towards EV-centered smart city power grids and increased employment of EMSs both for residential and commercial users, further investigation of such coordination frameworks is necessary and can yield significant techno-economic benefits to all stakeholders. There are multiple directions which can be pursued for research following up on this work, which are discussed in this section.

The objective of this paper to present the EMSs and the coordination framework between them from the point of power systems research. While the requirements for the information exchange have been presented, it is crucial to proceed towards implementing the information sharing platform. Ideally, this platform should be developed with a bottom-up approach, specifically designed to be employed for this purpose (such as the EMSs developed and presented in this paper). The topic of information sharing was briefly discussed in Section 2, specifically with regards to the limitation posed by the nature of day-ahead markets. This does not preclude from the fact that updating the schedules via frequent information exchange can (and indeed should) take place especially when high levels of uncertainty are foreseen. This should definitely be investigated in future work, and if possible, simultaneously implement a communication platform to leverage the benefits obtained from the coordinated operation of EVs.

Another prospect for future work is to conduct a global study with different electricity markets and work-culture differences. The conducted study was performed from a European perspective, however there is indeed a lot to be gained by analyzing the effect of such coordinated EMS employment under different conditions. An important factor that will be impacted by cultural and demographic differences will be the driving patters of EV owners. In this case, more complex probabilistic modeling of the EV commuting patterns such as the one presented in [24] should be employed to accurately capture the global differences and impacts on the employment of the proposed coordination framework.

Finally, different power grids can also be investigated, especially multi-microgrid networks and grids with decentralized operation. A more complex coordination mechanism between residential/commercial EMSs on one hand, and decentralized grid operation (specifically agent-based systems) is highly recommended for future work following-up on this study.

6. Conclusions

In this paper, an innovative coordination framework was proposed and implemented for different EMSs in a smart city with EVs. The model was conceptualized based on the coordination between individual HEMSs belonging to the EV owners and a PLEMS at their workplace. The HEMS only needed to share the EV arrival time at the PL, EV departure time from the PL, and arrival SoC. Meanwhile, the PLEMS shared each EV's departure SoC with its HEMS. Any extra information needed by the EMSs (e.g., PV forecasts, electricity market data, traffic data) was obtained through public cloud/web applications and repositories. The individual EMSs along with the proposed coordination framework was implemented and tested based on a real-life case study and by simulating a day-ahead operation. Two studies were performed. In the first, a power flow analysis was made to analyze the technical viability of the proposed approach. In the second, an economic analysis was made by calculating the electricity bill of an EV owner for a full working week under different scenarios of EMS operation. The results of both studies showed that the proposed EMS coordination framework was both technically beneficial for power grids and economically beneficial for the EV owners.

Appendix 1: HEMS User Preferences

The HEMS settings and user-defined preferences in Table A1 and A2 are the ones corresponding to the EV under study in Section 4.2. Since uncertainties are being considered by the proposed model, the EV preferences vary every for each day and EV being considered, according to the actual arrival time and arrival SoC of the day. The study performed in Section 4.1 used the same values in Table A1. The same EV has the same values as in Tables A2 and A3, however these values varied with each one of the 108 EVs under study according to the uncertainties modeled.

Table A1. Settings and user-defined preferences for the HEMS. The EV preferences are set according to the commuting schedule generated and is provided in Table A2 and Table A3.

Appliance	P_i	T_i	LB_b	UB_b	LB_S	UB_S
Dishwasher (1)	1.8	01:30	02:30	04:00	02:30	05:00
Washing Machine (2)	0.5	01:00	03:00	04:00	03:00	05:00
Clothes Dryer (3)	3.0	00:30	05:30	06:00	05:30	07:30
Living Room AC (4)	1.5	01:00	14:30	15:30	14:00	15:30
Microwave (5)	1.2	00:30	14:30	15:00	14:30	15:00
Laptop (6)	0.1	02:00	15:30	17:30	15:30	19:00
Cooker Hob (7)	1.5	00:30	14:30	15:00	14:30	15:00
Vacuum Cleaner (8)	1.4	01:00	04:30	05:30	05:30	06:00
Room AC (9)	1.0	00:30	16:30	17:00	17:30	18:00
Electric Vehicle (10)	*According to Generated Schedule as shown in Table I (Morning) or Table II (Afternoon)*					

Table A2. Resulting EV preferences for the HEMS with the morning schedule.

	P_i	T_i	LB_b	UB_b	LB_S	UB_S
Day 1	2.3	8:30	19:30	04:00	19:30	07:30
Day 2	2.3	7:00	20:30	03:30	20:30	08:30
Day 3	2.3	7:30	18:30	02:00	18:30	07:30
Day 4	2.3	8:00	19:30	03:30	19:30	06:30
Day 5	2.3	8:00	19:30	03:30	19:30	08:30

Table A3. EV preferences for the HEMS with the afternoon schedule.

	P_i	T_i	LB_b	UB_b	LB_S	UB_S
Day 1	2.3	6:00	19:30	01:30	19:30	07:30
Day 2	2.3	5:00	20:30	01:30	20:30	08:30
Day 3	2.3	5:30	18:30	00:00	18:30	07:30
Day 4	2.3	5:30	19:30	01:00	19:30	06:30
Day 5	2.3	5:30	19:30	01:00	19:30	08:30

Appendix 2: HEMS Operation for a Single Home (Morning Schedule)

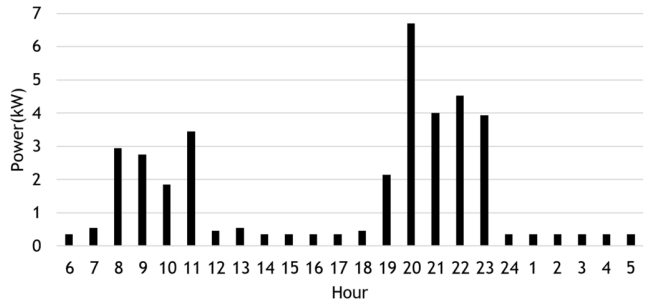

Fig. A1: Total demand for a single house (morning schedule) before HEMS implementation.

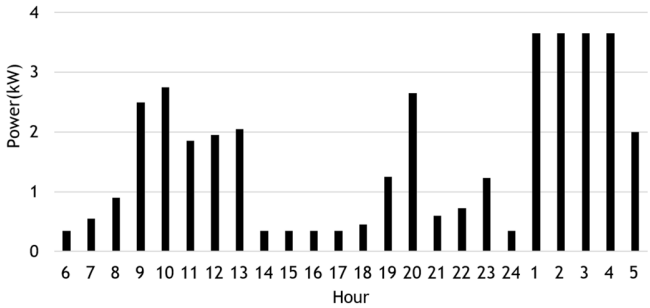

Fig. A2: Total demand for a single house (morning schedule) before HEMS implementation.

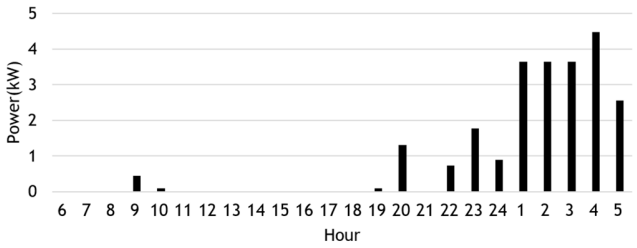

Fig. A3: Power injected from the grid to the home for a single house (morning schedule) after HEMS implementation.

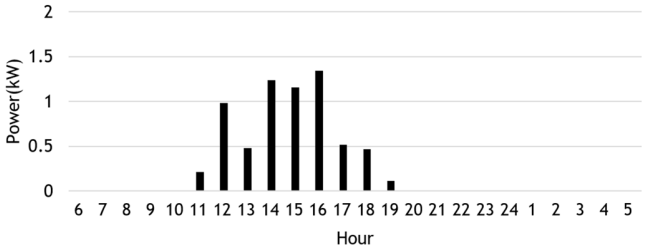

Fig. A4: Power injected from the home to the grid for a single house (morning schedule) after HEMS implementation.

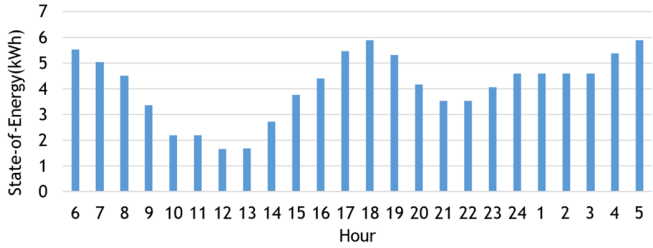

Fig. A5: Energy stored in the ESS for a single house (morning schedule) after HEMS implementation.

References

[1] Q. Duan, N.V. Quynh, H.M. Abdullah, A. Almalaq, T.D. Do, S.M. Abdelkader, M.A. Mohamed, "Optimal Scheduling and Management of a Smart City within the Safe Framework," *IEEE Access*, vol. 8, pp. 161847–161861, 2020.

[2] T. Qian, C. Shao, X. Li, X. Wang, M. Shahidehpour, "Enhanced Coordinated Operations of Electric Power and Transportation Networks via EV Charging Services," *IEEE Trans. Smart Grid*, vol. 11, no. 4, pp. 3019–3030, 2020.

[3] V. H. Nguyen, Q. T. Tran, and Y. Besanger, "SCADA as a service approach for interoperability of micro-grid platforms," *Sustain. Energy, Grids Networks*, vol. 8, pp. 26–36, 2016.

[4] H. Kikusato *et al.*, "Electric Vehicle Charge-Discharge Management for Utilization of Photovoltaic by Coordination between Home and Grid Energy Management Systems," *IEEE Trans. Smart Grid*, vol. 10, no. 3, pp. 3186–3197, May 2019.

[5] M. Lotfi, C. Monteiro, M. Shafie-khah, and J. P. S. Catalao, "Evolution of Demand Response: A Historical Analysis of Legislation and Research Trends," in *2018 Twentieth International Middle East Power Systems Conference (MEPCON)*, 2018, pp. 968–973.

[6] H. Zhang, Z. Hu, Y. Song, and Y. Song, "Power and Transport Nexus: Routing Electric Vehicles to Promote Renewable Power Integration," *IEEE Trans. Smart Grid*, vol. 11, no. 4, pp. 3291–3301, 2020.

[7] K. Kotsalos, I. Miranda, N. Silva, and H. Leite, "A horizon optimization control framework for the coordinated operation of multiple distributed energy resources in low voltage distribution networks," *Energies*, vol. 12, no. 6, 2019.

[8] M. Yousefi, A. Hajizadeh, and M. N. Soltani, "A Comparison Study on Stochastic Modeling Methods for Home Energy Management Systems," *IEEE Trans. Ind. Informatics*, vol. 15, no. 8, pp. 4799–4808, Apr. 2019.

[9] M.S. Javadi, A.E. Nezhad, P.H.J. Nardelli, M. Gough, M. Lotfi, S. Santos, J.P.S. Catalão, "Self-scheduling model for home energy management systems considering the end-users discomfort index within price-based demand response programs," *Sustain. Cities Soc.*, vol. 68, p. 102792, May 2021.

[10] A. Sangswang and M. Konghirun, "Optimal Strategies in Home Energy Management System Integrating Solar Power, Energy Storage, and Vehicle-to-Grid for Grid Support and Energy Efficiency," *IEEE Trans. Ind. Appl.*, vol. 56, no. 5, pp. 5716–5728, 2020.

[11] M. Yousefi, A. Hajizadeh, M. N. Soltani, and B. Hredzak, "Predictive Home Energy Management System with Photovoltaic Array, Heat Pump, and Plug-In Electric Vehicle," *IEEE Trans. Ind. Informatics*, vol. 17, no. 1, pp. 430–440, 2021.

[12] L. Zhang and Y. Li, "Optimal Management for Parking-Lot Electric Vehicle Charging by Two-Stage Approximate Dynamic Programming," *IEEE Trans. Smart Grid*, vol. 8, no. 4, pp. 1722–1730, Jul. 2017.

[13] S. Hussain, M. A. Ahmed, and Y. C. Kim, "Efficient Power Management Algorithm Based on Fuzzy Logic Inference for Electric Vehicles Parking Lot," *IEEE Access*, vol. 7, pp. 65467–65485, 2019.

[14] M. Shafie-Khah, P. Siano, D. Z. Fitiwi, N. Mahmoudi, and J. P. S. Catalão, "An innovative two-level model for electric vehicle parking lots in distribution systems with renewable energy," *IEEE Trans. Smart Grid*, vol. 9, no. 2, pp. 1506–1520, 2018.

[15] Y. Zhang and L. Cai, "Dynamic Charging Scheduling for EV Parking Lots with Photovoltaic Power System," *IEEE Access*, vol. 6, pp. 56995–57005, 2018.

[16] H. M. D. Espassandim, M. Lotfi, G. J. Osorio, M. Shafie-Khah, O. M. Shehata, and J. P. S. Catalao, "Optimal operation of electric vehicle parking lots with rooftop photovoltaics," in *2019 IEEE International Conference on Vehicular Electronics and Safety, ICVES 2019*, 2019.

[17] G.J. Osório, M. Lotfi, M. Gough, M. Javadi, H.M.D. Espassandim, "Modeling an electric vehicle parking lot with solar rooftop participating in the reserve market and in ancillary services provision," *J. Clean. Prod.*, vol. 318, p. 128503, Oct. 2021.

[18] M. Lotfi, T. Almeida, M. Javadi, G. J. Osorio, and J. P. S. Catalao, "Coordinated Operation of Electric Vehicle Parking Lots and Smart Homes as a Virtual Power Plant," in *Proceedings - 2020 IEEE International Conference on Environment and Electrical Engineering and 2020 IEEE Industrial and Commercial Power Systems Europe, EEEIC / I and CPS Europe 2020*, 2020.

[19] T. Almeida, M. Lotfi, M. Javadi, G. J. Osorio, and J. P. S. Catalao, "Economic Analysis of Coordinating Electric Vehicle Parking Lots and Home Energy Management Systems," in *Proceedings - 2020 IEEE International Conference on Environment and Electrical Engineering and 2020 IEEE Industrial and Commercial Power Systems Europe, EEEIC / I and CPS Europe 2020*, 2020.

[20] T. Yuvaraj, K.R. Devabalaji, S. Srinivasan, Natarajan Prabaharan, R. Hariharan, Hassan Haes Alhelou, B. Ashokkumar, "Comparative analysis of various compensating devices in energy trading radial distribution system for voltage regulation and loss mitigation using Blockchain technology and Bat Algorithm," *Energy Reports*, Sep. 2021.

[21] Entidade Reguladora dos Serviços Energéticos (ERSE), "Diretiva (extrato) 1/2020, 2020-01-17 - DRE." [Online]. Available: https://dre.pt/web/guest/pesquisa/-/search/128227680/details/normal?l=1. [Accessed: 22-Feb-2021].

[22] EDP Comercial, "EDP Comercial - Opções horárias." [Online]. Available: https://www.edp.pt/particulares/apoio-cliente/perguntas-frequentes/pt/contratos/novo-contrato/o-que-e-a-opcao-horaria-e-qual-a-melhor-para-mim/faq-4823/. [Accessed: 22-Feb-2021].

[23] REN, "SIMEE - Daily and Intraday - Prices." [Online]. Available: https://www.mercado.ren.pt/EN/Electr/MarketInfo/MarketResults/OMIE/Pages/Prices.aspx. [Accessed: 22-Feb-2021].

[24] M. P. Anand, B. Bagen, and A. Rajapakse, "Probabilistic reliability evaluation of distribution systems considering the spatial and temporal distribution of electric vehicles," *Int. J. Electr. Power Energy Syst.*, vol. 117, p. 105609, May 2020.